Novel "Breath Figure"-Based Synthetic PLGA Matrices for In Vitro Modeling of Mammary Morphogenesis and Assessing Chemotherapeutic Response

Thiruselvam Ponnusamy, Geetika Chakravarty, Debasis Mondal, and Vijay T. John**

Biodegradable poly(lactic-co-glycolic acid) (PLGA) porous films are developed to support mammary cell growth and function. Such porous polymer matrices of PLGA are generated using the easily implemented water-templating "breath-figure" technique that allows water droplets to penetrate the nascent polymer films to create a rough porous polymer film. Such breath figure-based micropatterned porous films show higher epithelial differentiation and growth than the corresponding flat 2D films, and represent the first instance of using them for tissue culture. Specifically, the breath figure morphology supports robust acinar growth with almost double the number of lobular–alveolar units compared to the 2D cultures. Gene profile analysis indicates that the cells grown on porous polymer films show enhanced expressions of mammary differentiation genes (GATA3, EMA, and INTEGB4) but lower the expression of mesenchymal gene (CALLA). Hormonal stimulation of these cultures dramatically increases expression of progenitor marker gene Notch1. Importantly, cells grown on porous PLGA films exhibit an enhanced resistance to doxorubicin treatment in comparison to 2D cultures. Breath-figure PLGA films show promise in mimicking in vivo mammary functions and can potentially be used to screen chemotherapeutic drugs. The simplicity and ease of fabrication of these polymer films is especially appealing to the development of effective biomaterials to support cell culture and differentiation.

1. Introduction

Postnatal mammary ductal development occurs during puberty through ramification of terminal end buds (TEB) to give rise to a ductal network consisting of luminal and myoepithelial cells. The luminal cells, as the name suggests, line the lumen of the duct, whereas the myoepithelial cells stay in direct contact with a laminin-rich basement membrane. This bilayered epithelium stays embedded in a fatty stroma. Hormonal changes during puberty, pregnancy, and lactation result in terminal differentiation of the ductal cells into milk producing acini.[1,2] The dynamic nature and complexity of mammary morphogenesis is a significant challenge when it comes to recapitulating this process in vitro. However, as most breast cancers arise in ducts from cyst-like structures that fail to differentiate into ductal and alveolar cells, it is paramount to develop in vitro model systems that recapitulate branching morphogenesis and retain all the essential features of a typical breast tissue including the stiffness afforded by the extracellular matrix (ECM).[1,3,4] These in vitro models are particularly needed to understand how improper differentiation can result in breast cancer growth, and to carry out meaningful screening of anticancer agents, which are effective against breast cancer cells and recapitulate their in vivo efficacies.

Traditionally, cells cultured in 2D petridishes have been used to evaluate the cytotoxicity of anticancer agents prior to testing in animal models and preclinical trials. However, cells grown on 2D surfaces lack the physiologically relevant microenvironment and the resultant cues emanating from reciprocal signaling between the epithelium and the underlying mesenchyme (fatpad) as seen in the breast tissue.[5,6] An emerging consensus therefore, is that traditional 2D cell culture may not accurately mimic the 3D environment in which cancer cells reside. Specifically, the unnatural 2D environment may produce inaccurate data regarding the predicted response of cancer cells to chemotherapeutics.[7] For instance, breast cancer cells grown in a 3D environment show a greater resistance to therapeutic agents, slower proliferation rates, different cell densities, reduced sensitivities to apoptosis, and distinct gene expression profiles in comparison to cells in 2D systems.[7–10] This is also true for ductal development where the formation of lumen and ductal structure is distinctly influenced by its 3D surroundings.[5,11,12] Such discrepancies between 2D and 3D cultures and the complexities of available animal models have prompted researchers to devise alternative in vitro model systems that are convenient,

T. Ponnusamy, Prof. V. T. John
Department of Chemical and Biomolecular Engineering
Tulane University
New Orleans, LA 70118, USA
E-mail: vj@tulane.edu
Dr. G. Chakravarty,[+] Prof. D. Mondal
Department of Pharmacology
Tulane University Health Sciences Center
New Orleans, LA 70112, USA
E-mail: geetikac@jonakee.com
[+]Present address: Jonakee Cancer Research, Inc., 5350 Bellaire Blvd., Bellaire, TX 77401, USA

DOI: 10.1002/adhm.201300184

reproducible, and possess relevant multifunctional and dynamic microenvironment characteristics.[13] Therefore, cultures that allow the growth of multi-cellular 3D structures and retain essential features of a typical breast tissue may be invaluable to drug development.

While the perfect method for 3D cell structures may not have been determined, clearly there is significant research effort in engineering inherently active biomaterial matrices that are reproducible, are commercially scalable and can produce the most in vivo-like structures possible. An additional focus has been to ensure that the biomaterial possesses biomechanical and biocompatible properties to support sufficient cell in-growth and differentiation to form living tissue-like structures. Furthermore, proper combination of signals delivered by biological growth factors and the ECM may be required for emulating in vitro a niche that can drive cells towards a defined phenotype.

Recently, 3D cultures of mammary cells in collagen gels,[3,14,15] commercial Matrigel,[3,16] chitosan scaffolds,[9,17] and micro-patterned arrays have been used extensively to replicate in vivo growth with varying degrees of success.[18] However, the matrix stiffness required to drive the commitment of mammary precursors to differentiated mammary architecture is lacking in these systems.[5] Here, we chose to develop porous films based on the FDA approved poly (lactic-*co*-glycolic acid) (PLGA50:50) polymer, which renders the necessary stiffness and pliability to regulate numerous cell functions. For this purpose, a "breath figure" technique has been utilized to create porous PLGA films with varied pore sizes. The breath figure mechanism is a simple way of producing porous structure with appropriate pore sizes highly interconnected with each other.[19] The porous structure is prepared under a controlled humid atmosphere (relative humidity ≥ 70%). The evaporative cooling effect of the polymer solution induces condensation of water droplets on the surface of a polymer solution, which, in turn, is self-packed, stabilized, and arranged into porous templates.[20–22] The topography with appropriate roughness and highly inter-connected multi-layered porous structure can facilitate cell adhesion, proliferation, differentiation in a natural manner.[11,23] These structures, also known as honeycomb-patterned polymer films have been shown to exhibit enhanced cell–cell adhesion and proliferation of NIH3T3 and HeLa cells in comparison to featureless flat films.[23,24] Recently, breath figure polymer films have also been investigated for supporting the growth of various cell lines, including hepatocytes, neural stem/progenitor cells, and endothelial cells. Tanaka and co-workers have reported the growth of human cancer cells on patterned polymer films.[25] However, breath figure structures have not been fully examined for any breast epithelial cell line including the most representative MCF-7 cells.[25,26] Based on the literature and the importance of developing materials for the culture of breast epithelial cell lines, our objective therefore was to evaluate PLGA-based breath figure polymer films for their influence on the growth kinetics, differentiation program, and the chemotherapeutic response of MCF-7 cells and compare these features to growth in a flat featureless surface environment.

Thus, in this paper, we describe the synthesis of various breath figure porous PLGA films fabricated with a spin-coating procedure to generate smaller pore structures and a dip-coating procedure to generate larger pore structures. MCF-7 cells cultured on these films show slower growth kinetics and a more differentiated phenotype compared to cells grown on 2D surfaces. We also demonstrate significant differences in their response to chemotherapeutic drug doxorubicin. Our findings indicate that these novel and engineered breath figure PLGA films may be an effective and alternative biomaterial to develop drug screening protocols against breast cancer cells and to recapitulate the branching morphogenesis seen in in vivo model systems of normal breast epithelial cells. The ease of fabricating such structures is the primary technology-based driving force for the research.

2. Results and Discussion

2.1. Engineering PLGA-Based Synthetic Film Using the Breath Figure Process

Our current understanding of tissue form, function, and their aberrant pathologies has evolved from 2D cell cultures, which often behave very differently from the 3D microenvironments of cells in animal model studies. It is becoming more and more apparent that the former approach is limited by considerable differences in morphology and differentiation program when cells are cultured in 2D substrates. Contrarily, animal studies are extremely time consuming and expensive. 3D culture techniques combine the flexibility and speed of tissue culture with tissue architectural cues afforded in vivo. It is no surprise therefore that several studies have attempted to build 3D models for mammary morphogenesis using various types of extracellular matrix (ECM) components. However, to date, only a few studies have tried to use purely synthetic scaffolds for mammary morphogenesis.[8,17,27] We describe here, our efforts to design and engineer synthetic microporous polymer films that faithfully recapitulate the in vivo microenvironment of breast tissue. The objective was to choose biopolymers that can influence cell adhesion, polarity, and induce cellular differentiation of mammary cells. Other considerations were biocompatibility and biodegradability, topography, and mechanical properties. The porosity of the biomaterial was another major factor that was varied to assess how it influenced mammary cell growth and differentiation. **Figure 1** describes the fabrication of PLGA breath figure-based polymer films. Besides the biodegradability of PLGA, the simplicity of forming pores in such materials using the breath figure method makes these structures viable candidates for biocompatible matrix construction.

SEM characterizations of the spin-coated breath figure porous PLGA film revealed that the surface of the polymer (**Figure 2**A) is filled with pores throughout the large surface area of the film with an average pore size dimension of 4.8 ± 2.6 μm. The formed micro-porous polymer matrix closely resembles the stiffness of ductal architecture and the tumor microenvironment in vivo. The pores on the surface provide a large surface area for better cell–cell adhesion, whereas the presence of inter-connected pores allows infiltration of cells and diffusion of organic nutrients into the bulk polymer to induce cell–matrix interactions.[10] In the breath figure process, pore formation is not restricted to the surface alone.

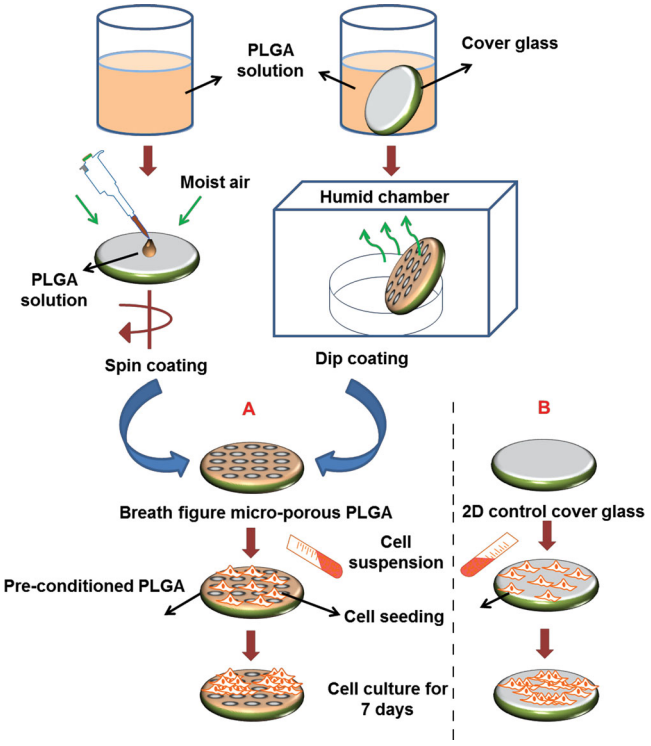

Figure 1. Experimental setup illustrates the fabrication of breath figure PLGA and cell culture on these porous films in vitro. Two different pore sizes were obtained simply by altering the fabrication procedure. Under constant humid condition, the PLGA solution was quickly evaporated out in the spin coater to form pores in the range of 2–12 µm. However, in the dip coating, the slow evaporation of PLGA solution produced pores in the range of 5–30 µm. A) The scheme illustrates the MCF-7 cells seeding onto the porous polymers (regardless of pore sizes). The samples were preconditioned with the cell culture medium overnight prior to cell seeding. After 7 d of cell culture, the formation of 3D tissue-like structure is depicted in the schematic diagram. B) When the cells are seeded in 2D control cover glass (no polymer coating), the cells grow as monolayer on the surface.

Instead it is also prevalent in the bulk phase as a multilayered porous network. A cross-sectional view in Figure 2B better illustrates the nature of the inter-connected porous structure. As stated by Bolognesi and co-workers, formation of such multi-layered porous structure in the bulk phase is mainly due to the interfacial energy interaction, which allows the water droplets to sink into the polymer film during the evaporative cooling of breath figure process.[20] For the PLGA–dichloromethane system, we have reported earlier the formation of such porous structures in the bulk polymer.[21] Figure 2C,D show the SEM images of surface and side view of the spin-coated non-porous PLGA film. As expected, the surface of the non-porous film completely lacks porous structures. This may be due to the fact that the non-porous film was fabricated by purging nitrogen gas (<10% humidity) into the spin-coating chamber. Under the inert atmosphere, the solvent evaporates out quickly and creates a film with no condensation of water droplets. When compared to the opaque natures of the spin-coated porous breath figure PLGA, the non-porous 2D films obtained were transparent with virtually no pores or ridges on the surface.

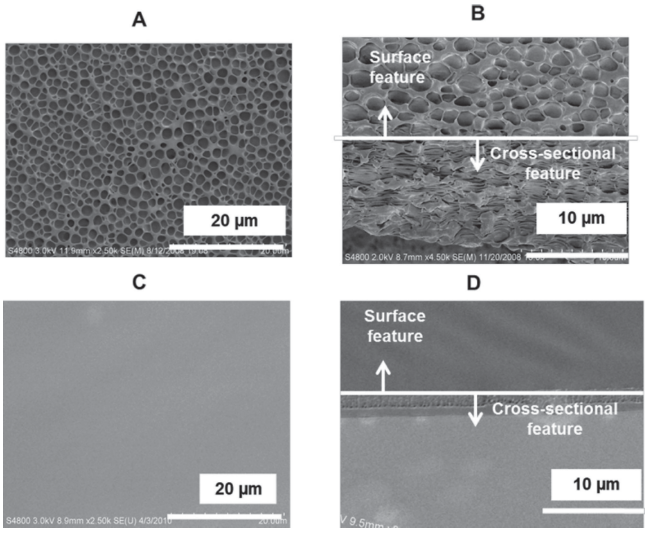

Figure 2. Scanning electron microscopy (SEM) images of spin-coated porous and non-porous PLGA films. A,B) Surface and cross-sectional view of spin-coated porous PLGA. 10% (w/v) PLGA solution dissolved in dichloromethane was spin-coated at 2500 rpm for 30 s under constant humid air stream. The breath figure PLGA coatings obtained were opaque and highly porous (average pore size 4.80 ± 2.6 µm) in nature and the side view showed the presence of inter-connected and multi-layered pores in the bulk polymer phase. C,D) Surface and cross-sectional morphology of spin-coated non-porous PLGA film. The film was obtained by spin coating the 10% (w/v) PLGA solution under N_2 gas stream. Under dry atmosphere, the films obtained were transparent and flat with no porosity either on the surface or bulk phase.

2.2. Porous Architecture and Roughness of the Spin-Coated Breath Figure PLGA Supports Enhanced Morphogenesis of Breast Epithelial Cells

To further assess if the porous architecture of the spin-coated PLGA film is indeed a better substrate to support functional growth, MCF-7 cells were cultured on spin-coated PLGA, non-porous PLGA film, or glass cover slips for 7 d, and stained with toluidine blue. Morphological assessment and acinar growth were scored to compare growth among the three surfaces. Phase contrast imaging showed that cells adhered well and spread as a thin single layer of cells on the glass surface (**Figure 3**A) with little if any cell aggregation on the surface. The same was true for growth on the 2D non porous PLGA film (Figure 3B). Cell shape in these 2D systems was observed to be stretched and spindly. On the other hand, cells grown on the spin-coated porous PLGA film demonstrated distinct 3D growth demonstrating round and well-developed cell aggregates with features of branching morphogenesis (shown with arrows) and lobulo alveolar growth (shown with asterisk), (Figure 3C,D). These morphological features are characteristic of typical human luminal epithelial cells in vivo. The lobular units in porous PLGA films varied in size with a range of 100–300 µm. Notably, even though the volume of toluidine blue solution used for staining of 2D and breath figure samples was the same, the images in Figure 3 suggest that the uptake of dye solution is much higher in the porous spin-coated samples as compared to 2D flat samples (cover glass and

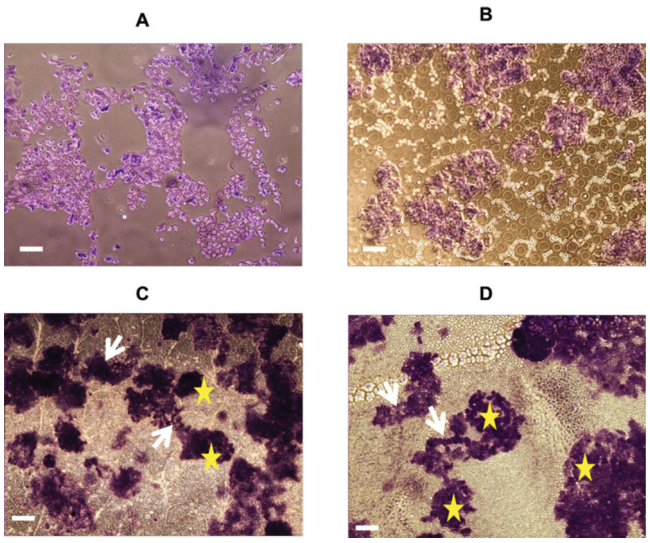

Figure 3. Morphological analysis of MCF-7 cells cultured for 7 d on 2D controls and spin-coated breath figure PLGA. Staining procedure: Toluidine blue (scale bar indicates 100 µm). A) Toluidine blue staining shows monolayer growth of cells in 2D cover glass. B) represents the staining on 2D non-porous PLGA film. The cell growth pattern was more or less similar to 2D glass with little aggregation of cells on the surface. The flat film does not render micro-environmental roughness characteristics to support cell proliferation and differentiation. Instead, the cells adhered and proliferated as a monolayer structure. C,D) Photomicrographs of two different fields showing cell growth on porous spin-coated PLGA. The growth was clearly 3D with large number of cell aggregates and clusters. Formation of elongated branched ductal and alveolar structure (arrowhead indicates duct-like structure, asterisk indicates lobular-alveolar structure) are typical characteristics of mammary gland.

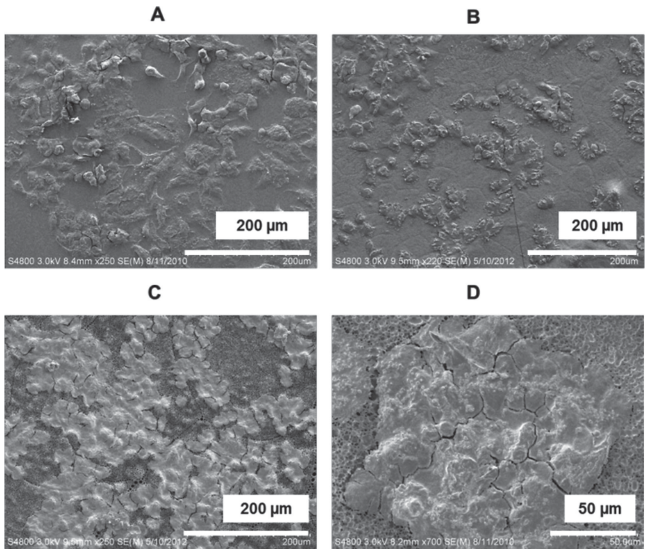

Figure 4. SEM of MCF-7 cells cultured on 2D systems and spin-coated breath figure PLGA. A,B) Surface topography of fixed MCF-7 cells cultured on 2D cover glass and 2D flat PLGA film, respectively. Following fixation of cells, the samples were air-dried and subjected to gold sputtering prior to SEM imaging. The images confirmed the monolayer distribution of MCF-7 cells grown on 2D samples. C,D) Low and high magnifications of cells grown on spin-coated patterned PLGA. The porous structure supported the adhesion of cells and guided them to proliferate as multilayer aggregation of cells.

non-porous PLGA). Perhaps, the large surface area of the porous PLGA allows accommodation of larger cell aggregates in a confined space, which results in increased uptake of staining solution. In the case of flat substrates, cells attach and proliferate as a single layer of sheet along the surface and thus do not accumulate as much dye. It is important to mention here that even though there is precedence for use of ECM-coated glass coverslip for 2D culture studies, the use of common reagents like collagen, fibronectin, or PEG to coat the glass coverslip was deliberately avoided in this study as our objective was to study the native response of these cells in the two different microenvironments. Moreover, these agents tend to produce strong background staining that interferes with subsequent imaging. Additionally, since MCF-7 cells independently secrete enough matrix, not treating the cover glass with extracellular matrix had no influence on their attachment and growth.

SEM analysis further substantiated our observations from phase contrast microscopy. The SEM images in **Figure 4** show the monolayer distribution and elongated phenotype of MCF-7 cells growing on glass cover slips and on non-porous PLGA film surfaces (Figure 4A,B). However, in the case of spin-coated porous PLGA film, cells were arranged as clusters and grew on top of each other as seen in Figure 4C (low magnification) and Figure 4D (high magnification). Overall, the comparative analysis of growth in 2D and spin-coated porous PLGA film suggests that the presence of porosity in the spin-coated PLGA greatly influences the cell behavior and directs the cell to sense the surrounding microenvironment.[28] The increased cell–cell and cell–polymer matrix interactions are able to promote proliferation and differentiation of MCF-7 cells into defined functional units. However, when cultured for longer duration, MCF-7 cells were attached mainly on the surface of the patterned PLGA utilizing the roughness on the topography and large surface area of microcavities, and no significant growth of cells was observed in the bulk PLGA phase. This may be due to the fact that the average pore size of the spin-coated PLGA (4.8 µm) was less than the size of MCF-7 cell (6–8 µm) and hence allowed only nominal growth inside the films.[29]

2.3. Endogenous Web-Like Porous Pattern of the Dip-Coated PLGA Facilitates Branching Morphogenesis

To assess if increasing the pore size, would allow more robust growth in the bulk phase, we modified the coating procedure in the breath figure process. Instead of spin-coating where the solvent is quickly evaporated off, we sought to dip coat the substrate so that the solvent is vaporized slowly in the presence of humid air. **Figure 5**A,B show low- and high-magnification SEM images of dip-coated porous PLGA films. Compared to spin coating, the average pore dimension of dip-coated PLGA films was 15.28 ± 5.2 µm. Figure 5C shows the pore size distribution plot for both types of film. For dip-coated porous PLGA, more than 65% of pores were formed in the size range of 12–30 µm. Contrarily,

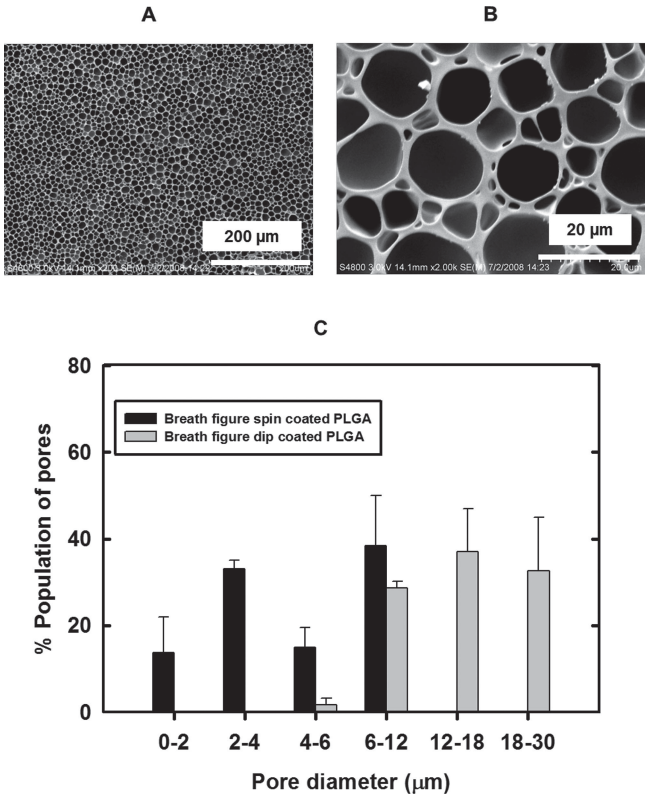

Figure 5. A,B) Low- and high-magnification SEM images of dip-coated porous PLGA. Unlike spin-coated porous PLGA, the dip coating produced larger pores and the pore size were in the range of 5–30 µm. The average pore size measured was 15.28 ± 5.2 µm. C) Comparison of percentage population of pores measured for both spin- and dip-coated samples. Using Image J software, we recorded 300 pores from at least five SEM images from three different experiments ($n = 3$). Each pore was measured for pore size. Compiled average pore size and distribution in over the range 0–30 µm are shown in the plot. More than 65% of pores were in the range of 12–30 µm for dip-coated samples. In contrast, 50% of pores were in the range of 4–12 µm for the spin-coated samples.

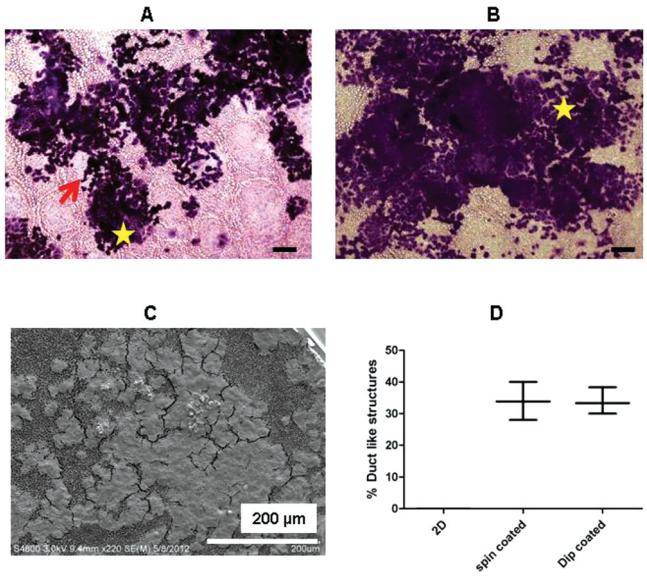

Figure 6. A,B) Low and high magnification of morphological development of MCF-7 cells cultured on dip-coated porous PLGA. Toluidine blue staining shows the robust growth of cells differentiated into duct-like (shown in arrows) and lobular-alveolar structures (shown in asterisk). The larger pore size of dip-coated PLGA facilitates the cells to infiltrate into the bulk phase and the size of lobular-alveolar structure is increased significantly as compared to spin-coated porous PLGA. Scale bar denotes 100 µm. C) SEM image of corresponding morphology of MCF-7 cells fixed and gold coated after 8 d of cell culture. D) Quantitation of percent duct-like structures in 2D cover glass, spin- and dip-coated cultures. Compared to 2D cover glass, ductal growth is highly significant on spin- and dip-coated PLGA films ($p < 0.0001$, Dunnett's multiple comparison test). Experiments were conducted three times and for each experimental condition, five random fields were imaged and analyzed for% ductal growth (% ductal growth = [(no. of ducts)/(no. of ducts + no. of lobular–alveolar structures)×100].

the spin-coated porous PLGA exhibited only 50% of pores in the 4–12 µm range. Similar to the spin-coated porous PLGA, cells seeded on the dip-coated porous PLGA grew into well-defined ductal and lobular structures and showed clear mammary epithelial cell morphology (**Figure 6**A,B). We also confirmed through SEM that the cells not only form aggregates (Figure 6C) but also grow in the bulk phase. To assess whether the synthetic dip-coated porous PLGA films steered the growth of MCF-7 cells towards acinar morphology and induced branching morphogenesis, cells plated in 2D cover glass were compared with cells grown on patterned dip coated PLGA. After 8 d in culture, they formed cysts-like structures, which were spherical and glandular in appearance and contained a hollow lumen with many cellular processes arising from the basal surface of the cystic growth. The term "branching," is being used to describe the tubular processes as they resemble the structures that form during mammary morphogenesis in vivo.[30,31] These cultures also showed lumen-containing lobular structure. On the contrary, 2D cultures showed only monolayer growth except at the edges, where occasionally some overlaying of cells was observed. Notably, the branching phenotype of the cyst-like structure was observed as early as day 5 of culture but was strongest around day 8–10. But due to substantial increase in cell death by day 10, culture timings were limited to 7–8 d for most studies where quantitative measurements were undertaken.

Quantitation of duct-like and lobular–alveolar structures showed that the average percentile of duct-like structure (Figure 6D) obtained for both patterned spin- and dip-coated PLGA films was similar (36.8% and 33.9%, respectively); however, the lobulo-alveolar units on dip-coated PLGA films were 1.88 times larger in comparison to the structures observed on spin-coated porous films. Furthermore, even though the difference in percentage of ductal outgrowth between spin- and dip-coated PLGA films was not statistically significant ($p > 0.05$), this difference was highly significant when the out-growths on porous PLGA films were compared to percent ductal growth in 2D cover glass ($p < 0.01$). We next asked could this significantly different response stem from differences in ECM cross-linking and stiffening within the two environments.

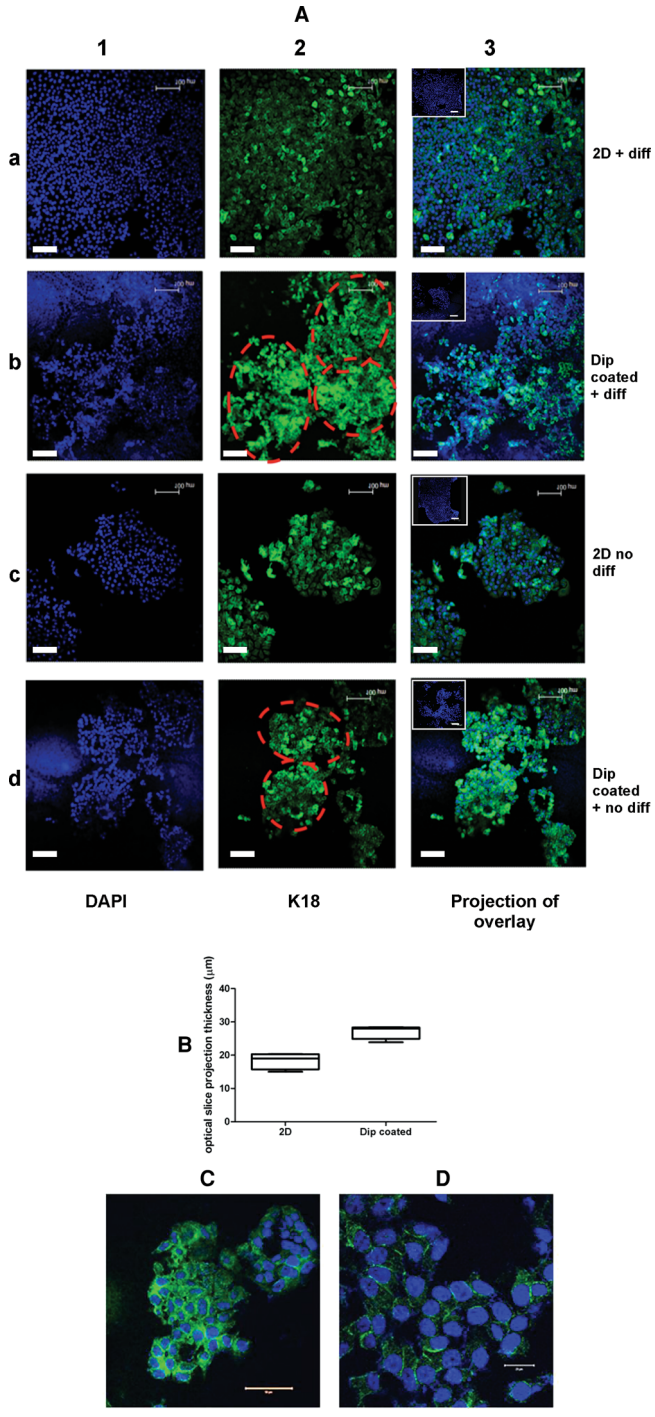

Figure 7. Micropatterned polymer films support more robust lobulo-alveolar 3D growth with or without mammary differentiating agents. Scale bar indicates 100 µm. A) Confocal imaging of K-18 stained MCF-7 outgrowths on 2D glass coverslips (panels a_1 to a_3 and c_1 to c_3) and dip coated porous PLGA (panels b_1 to b_3 and d_1 to d_3) after a week of culture in the presence (rows a and b) or absence (rows c and d) of differentiating agents as described in the methods sections. Lobulo-alveolar acini and ductal outgrowths occupied almost whole of the PLGA matrix but were not observed in 2D glass coverslip cultures. The structures encircled with red broken dashes identify lobulo-alveolar acini. The stained specimens were imaged simultaneously at two different excitation wavelengths (405 and 488 nm) using a single krypton/argon laser to obtain individual optical sections at high resolution in sequence through the thickness of the specimen. Column 1 represents a z-series projection of nuclei stained with DAPI (blue). Column 2 represents the corresponding z-series projection of lobulo-alveolar acini stained with K-18 and visualized using Alexa 488 secondary antibody (green). Column 3 represents a z-series projection overlay of DAPI and Alexa 488 staining. The no antibody controls are shown as insets in the projection overlay panel. Photomicrographs are representative of at least three different experiments. B) Histomorphometric quantitation of optical thickness of the outgrowths on 2D and dip- coated patterned PLGA films stained with DAPI and K-18. $n = 4$ fields of view from independent experiments. The average thickness of 3D outgrowths was found to be 1.5 times that of cells cultured in 2D systems. This was validated by the significantly different medians ($p = 0.0286$, two tailed Mann-Whitney test) of the two groups of outgrowths. C) shows a confocal laser scanning microscope image of E-cadherin/DAPI double immunofluorescence-stained mammary outgrowths from breath figure PLGA films, showing lumen containing acini with distinct apico-basal expression of E-cadherin. D) shows E-cadherin/DAPI double immunofluorescence-stained mammary outgrowths from 2D glasscover slips. Photomicrographs are representative of two independent experiments. Cells grown on PLGA films show strong cell adhesion and maintain proper polarity compared to the control cells grown on glass coverslips.

2.4. Pattern of K18 and E-Cadherin Expression Confirm the Polarized Ductal/Acinar Structure of the Outgrowths in Dip-Coated PLGA Films

ECM signaling has been shown to drive the cellular changes, which sculpt tissues and organs during embryogenesis.[32,33] For the same reasons, abnormalities in the mechanical environment of epithelial tissues can contribute to their malignant transformation and progression.[34] Conversely, exposure of cancer cells to microenvironments of a healthy tissue should help their transition to more normal differentiated phenotype.[35] To investigate this issue, we asked whether the dip-coated porous PLGA films with relatively large porous matrices would provide an environment where mammary cells could lay down their own matrix, make their own autocrine and paracrine regulatory factors, and steer the growth of epithelia in a stereotyped pattern to form ducts and luminal structures even in the absence of differentiating agents.

In order to test whether the porous matrix of the dip-coated PLGA supported branching morphogenesis and luminal growth, confocal analysis of 2D and dip-coated films was performed (**Figure 7**A). Ductal/acinar attributes of the outgrowths were ascertained with expression of lineage specific ductal and luminal markers K18 and distribution of epithelial-Cadherin (E-cadherin). These proteins were revealed by green fluorescence. The relatively more porous dip-coated matrix showed intense K18 positive ductal branching outgrowths with lumens (Figure 7A panels b and d) as compared to the flat growth in the 2D control cover glass systems (Figure 7Aa,c). Consistent with our predictions, significant deeper in-growth of the branched cystic structures was recorded in the dip-coated breath figure films ($p = 0.02$, Mann–Whitney test, Figure 7B). Based on these results, we also examined how larger pore size of the dip-coated PLGA film may affect ductal polarity of MCF-7 outgrowths. Our rationale to particularly investigate changes in polarity was based on earlier reports that have shown that in the right context, either due to an injurious insult or environmental

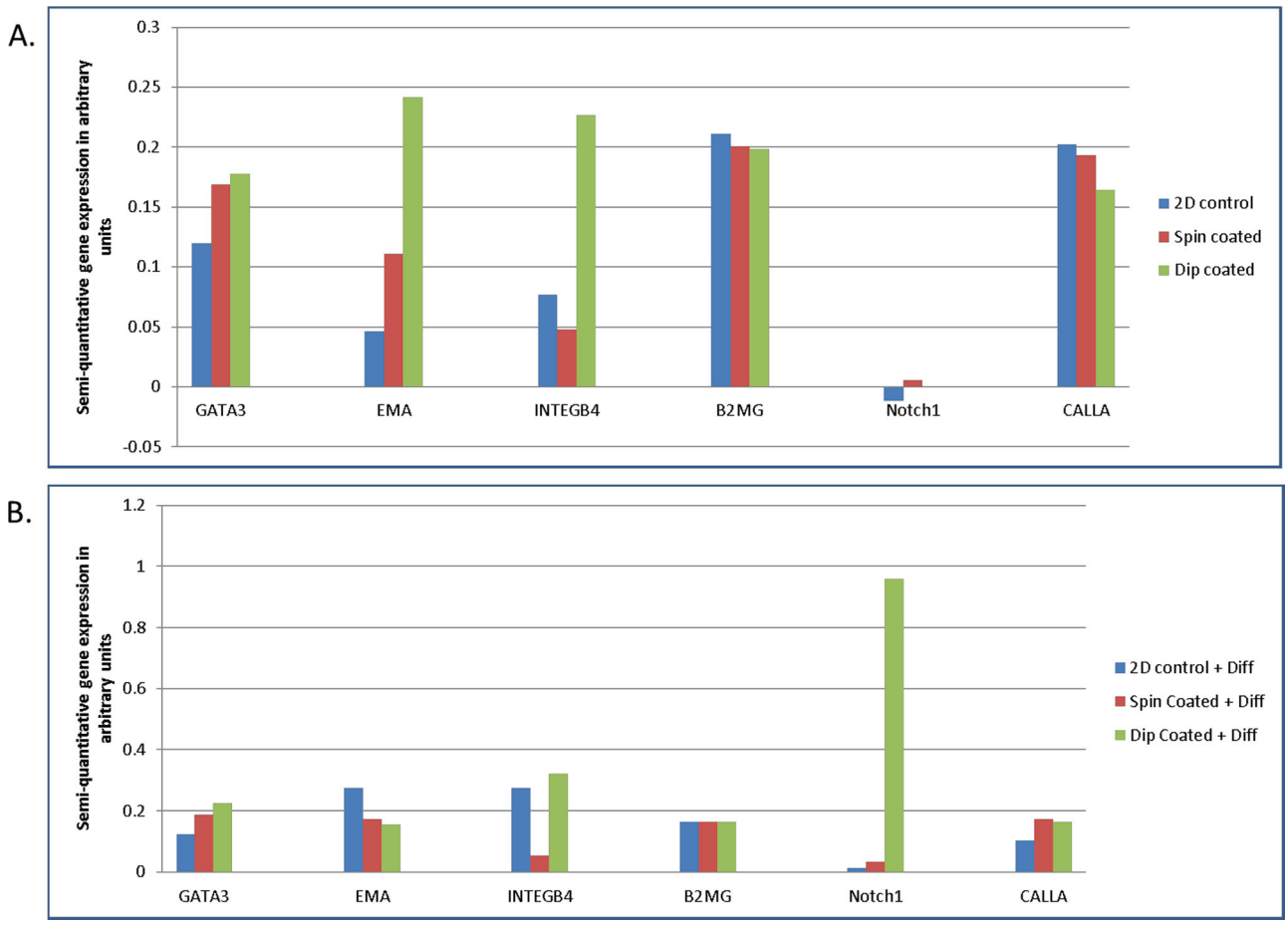

Figure 8. Representative plot of semi-quantitative RT-PCR expression data of *GATA3*, *EMA*, *INTEGB4*, *B2MG*, *Notch1*, and *CALLA*. The expression of these genes was quantitatated with GelQuant.NET v 1.7.8 provided by biochemlabsolutions.com. The expression of genes involved in mammary differentiation and progenitor cell specification is altered when cells are grown on breath figure PLGA films either in the A) absence or B) presence of differentiating agents [dexamethasone (1×10^{-6} M), hydrocortisone (1 μg mL^{-1}), insulin (5 μg mL^{-1}), and prolactin (10 ng mL^{-1})].

perturbations, the breast cancer epithelium may become activated and primed for induction of epithelial plasticity and undergoes epithelial–mesenchymal transition (EMT). This transition is usually accompanied by loss of E-cadherin expression and apico-basal polarity. However, if our hypothesis that cystic growth in the porous environment of the dip-coated PLGA may allow for deposition of a cell's own ECM and growth factors, then one would expect to see no loss of E-Cadherin or apico-basal polarity. Indeed our data on the expression of E-cadherin revealed that ductal/acinar outgrowths maintained an epithelial phenotype including correct apico-basal polarity and cell–cell adhesions (Figure 7C,D). Quantitation of the dip- and spin-coated cultures showed that more than 80% of outgrowths showed normal, ductal morphology, as opposed to less than 5% in 2D non porous films that too mostly confined to the edges. But contrary to our expectations, cultures grown on the porous PLGA microenvironment did not show significant differences in acinar growth with or without the differentiating agents (Figure 7A, compare panels b and d). To gain a better understanding of the subtle differences in bio-molecular nature of the differentiated phenotype of the cystic acinar outgrowths that may have been missed by the gross morphometric analysis, RT-PCR analysis of some known lineage specific mammary differentiation genes was undertaken.

2.5. Distinct Phenotype of 2D and Porous PLGA Outgrowths at the Molecular Level

As shown in **Figure 8**A, RT-PCR analysis identified a significant increase in GATA3, EMA, and Integrin β4 transcripts mainly in the porous PLGA outgrowths. Expression of all three of these genes has been associated with luminal differentiation, further confirming that outgrowths of breast cancer cells in the porous PLGA microenvironment acquire a more differentiated phenotype. However, contrary to published reports that suggest EMA expression to be high in ductal/acinar outgrowths, we observed its expression in both 2D and porous PLGA platforms. An explanation for its expression in both types of culture conditions may be that EMA is also known to be expressed in bipotent progenitor cells suggesting that both luminal and more spindly mesenchymal progenitor cells may express it. We therefore considered the possibility that in addition to exhibiting differences in inducing luminal lineage genes, the

PLGA matrices may also differ in their ability to induce progenitor cell-specific genes. As no mammary specific progenitor cell markers are known, we sought to study the expression of NOTCH-1 based on its role in hematopoietic stem cell renewal and differentiation. Consistent with our hypothesis expression of NOTCH-1 was seen only in response to hormonal stimulation and only in cells growing in the porous microenvironment of the breath figure polymer films (Figure 8B). These data suggest that the outgrowths from 2D and patterned PLGA films were indeed distinct from one another at the molecular level. Additional evidence of molecular differences in progenitor specific gene expression came from expression of myoepithelial marker CALLA. As shown in Figure 8A, expression of CALLA is decreased in cells cultured on spin- and dip-coated films in comparison to 2D cover glass cultures. However, hormonal stimulation increases its expression (Figure 8B) in the patterned PLGA subgroup, suggesting that these matrices can induce signaling from the ECM to nucleus to regulate gene expression and functional changes in response to differentiating agents.

It may be worthwhile to mention here that our attempt to reproduce the RT-PCR data with qPCR were unsuccessful as many of the genes under study have naturally occurring alternatively spliced variants or frame shift variants. These variant transcripts result in more than one amplicon and hence erroneous quantitative outputs.

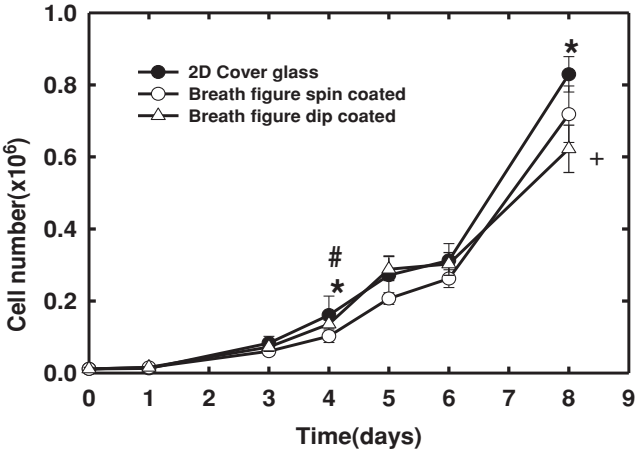

Figure 9. Growth proliferation kinetics of MCF-7 cells on micropatterned dip-, spin-coated, and 2D glass cover slips. The overall cell growth was higher in 2D system in comparison to porous polymers after 8 d of cell culture. Significant statistical difference in cell proliferation was noted between 2D and spin-coated samples (Student *t*-test $*p < 0.05$). For day 4, no statistical difference was observed between 2D and dip-coated samples ($\#p > 0.05$). However, by day 8, there was a significant difference in the growth kinetics between cells grown on 2D and the polymer systems. High statistical difference was observed between 2D and dip-coated samples ($p < 0.01$). Initial cell seeding density = 25 000 cells/well. Experiment was conducted in triplicate and data plotted as mean ± SD.

2.6. Growth Proliferation of MCF-7 Cells on Breath Figure PLGA and 2D Substrates

The morphological changes triggered by the interaction between the microenvironment of a porous polymer matrices and MCF-7 cells led us to ask whether the spin- and dip-coated PLGA can support the recovery and proliferation of cells seeded after trypsinization just as cells in 2D do. To address this question, we seeded 2.5×10^4 MCF-7 cells/well on preconditioned porous PLGA samples (both spin coated and dip coated) and on the control glass coverslips (**Figure 9**). The plates were observed daily under a standard light microscope. It is an empirical task to look for cell proliferation on the patterned polymer films as the cells migrate into the porous architecture of these films, necessitating repeated trypsin treatment to release all the cells before counting. Quantitation of number of cells demonstrated that patterned dip- and spin-coated PLGA had a 56- and 64-fold increase in cell density at the end of the 8 d culture period, respectively. As expected, growth was even higher in case of 2D cover glass, where a 74-fold increase in cell density was observed.

Although we seeded a very small number of cells on day zero, clusters of proliferating MCF-7 cells were formed routinely on these polymer films. We speculate that both the interaction of cells with the microenvironment of the porous matrix and the cell density provide a conducive environment for cells to proliferate initially. This is clearly illustrated in the graph in Figure 9. However, even though the graph reveals a progressive increase in the number of cells as a function of time, supporting the notion that trypsinized cells seeded onto the polymer films are able to recover and grow; growth at later time points starts to plateau and eventually starts to slow down (growth on days 5 and 6). The initial increase in proliferation at earlier time points may be because of the porous nature of the polymer matrix and low cell density. These attributes allow MCF-7 cells to possess morphological features of regularly dividing spindly cells instead of their expected growth as clusters in rough surface of the polymer. However, once they started to grow as clusters at later time points and cell matrix communications are established, cell proliferation slows down to allow differentiation to commence (as evidenced from our other experiments as well). In contrast, cells on 2D continued to proliferate all through the duration of the experiment. Our data suggest, trypsinized MCF-7 cells are able to recover in the porous matrix of the spin- and dip-coated PLGA and that cell density and cell matrix interactions together influence proliferation and differentiation of cells in breath figure polymer films.

2.7. Cells Grown on Porous PLGA Polymer Films Show Increased Resistance to Doxorubicin Treatment

We observed that culturing MCF-7 cells in breath figure polymers produces distinctly different proliferative and differentiation responses than when cultured on standard 2D glass coverslips. Additionally, we now know that the move to the porous PLGA culture platform yields very different transcription levels of some of the known differentiation genes. In order to assess how this difference in biomolecular behavior in the different microenvironment affects the response of these cells to pharmacological agents, we treated MCF-7 cells grown on the 2D cover glass and on spin- and dip-coated polymer films with doxorubicin

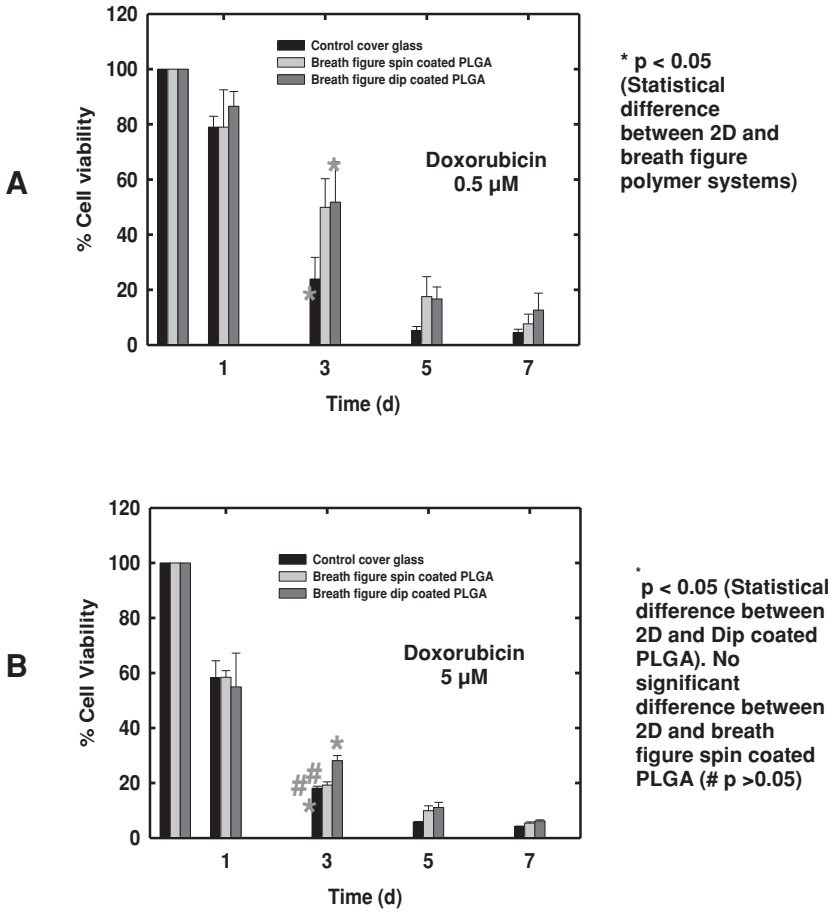

Figure 10. Doxorubicin treatment for MCF-7 cells grown on 2D control and breath figure PLGA films. Percent cell viability was plotted over time after exposing the MCF-7 cells cultured on 2D controls or porous polymers every 72 h with A) 0.5×10^{-6} M or B) 5×10^{-6} M doxorubicin. Viable cells were measured using the standard alamar blue proliferation assay. In comparison to 2D controls, both spin- and dip-coated PLGA systems exhibit resistance to doxorubicin. At the end of day 3 treatment, 55% of plated cells were viable in patterned films group, whereas only 20% viable cells were present in 2D controls. Statistically, the obtained mean values were significantly different between 2D and polymer samples (Students *t*-test $*p < 0.05$). Increasing the drug concentration level to 5×10^{-6} M shows no appreciable difference in toxicity effect between 2D and patterned polymer group.

(0.5 and 5.0×10^{-6} M). Doxorubicin is an anthracycline antibiotic that is currently considered to be one of the most effective agents in the treatment of breast cancer.[36,37] The response of cell proliferation to the drug treatment was evaluated using the alamar blue cell viability method.[38] From the absorbance values measured, the percentile cell viability was determined by normalizing the data with DMSO treated (no drug treatment) controls. As seen in **Figure 10**A, the response of MCF-7 cells growing as a 2D monolayer and exposed to 0.5×10^{-6} M doxorubicin is such that by day 3 of treatment there are only 20% viable cells. However, there is ≈55% survival in the porous PLGA polymer group, suggesting that doxorubicin is less effective on cells grown on the porous PLGA polymer films. When the growth response to doxorubicin in the 2D group is compared to growth response in PLGA polymer group, the difference is statistically significant ($p < 0.05$) and is to be anticipated from the reduced proliferation and enhanced differentiation activity observed in these microenvironments. Moreover, cells in 2D grow homogeneously with an adequate supply of nutrients and no barrier for diffusion of drug components. Contrarily, the reduced sensitivity to doxorubicin in the PLGA environment is influenced by the porous microenvironment, which replicates the in vivo physiological milieu of heterogeneity ranging from reduced diffusion of nutrients, hypoxia, and increased cell–cell and cell–polymer matrix interactions. Overall, our results correlate well with previous reports that have shown that tumor cells grown in 3D cultures are more resistant to chemotherapy agents as compared to 2D cultures. However, treatment with higher concentrations of doxorubicin ($>5 \times 10^{-6}$ M) (Figure 10B) showed little difference in behavior because at these high concentrations the drug was immediately toxic to cells.

3. Concluding Remarks

The use of PLGA in the biomedical field is well known for drug delivery and tissue engineering applications because of the convenience to modify its properties including degradation characteristics.[39,40] However, as PLGA degrades hydrolytically and releases monomers that are absorbed into the body metabolism with no toxic remnants, the simple fabrication of breath figures as described in this study adds to the class of novel designed biocompatible materials

This paper provides a quantitative understanding of the role of synthetic polymer microenvironments in altering cellular behavior; in particular, the changes in morphology, proliferation, differentiation, and response to pharmacological intervention in 2D and micropatterned rough environments. A simple breath figure method was exploited to generate broad range of pores (between 2 and 30 μm) in thin biodegradable PLGA polymer films. These films are quite robust and can be handled with no danger of mechanical tear or rupture. These porous polymers were inoculated with MCF-7 cells and their morphological characteristics were assessed through toluidine blue staining, confocal analysis, and scanning electron microscopy. The cells cultured on porous PLGA polymers clearly demonstrate functional growth as evident through the development of branched ductal structures, lobulo alveolar growth and changes in gene expression. Increasing the porosity of PLGA films by dip coating supports more robust growth of these cells resulting in the formation of much larger lobular-alveolar structures. MCF-7 cells in this microenvironment demonstrate a slower proliferation rate and increased differentiation in comparison to cells grown on spin-coated porous PLGA films or as 2D cultures. The increased porosity of dip-coated films provides a large surface area and microenvironmental topographical features for the aggregation

of a large number of cells in 3D orientations resembling the in vivo mammary function. The growth response of cells to doxorubicin is comparable to the in vivo systems, as the cells grown on rough PLGA matrices are more resistant to the therapeutic agent. More importantly, these breath figure PLGA polymer films are biocompatible and this could pave the way for them to be used to culture multiple cell types leading to a better understanding of cellular behavior and differentiation. The materials have potential in the preparation of in vitro tumor mimics that can be used to study response to drug treatment. In recent years, there has been a significant increase in the design of novel materials that have been shown to provide support for cell growth and differentiation including the soft-functionalized hydrogels developed by Werner and co-workers.[41,42] It is envisaged that the ease of fabrication of breath figure PLGA structures will add to the class of such useful and biocompatible supports.

4. Experimental Section

Materials and Cell Culture: Poly (D,L-lactide-*co*-glycolide) (PLGA 50:50) polymer (Resomer RG 506) was purchased from Boehringer Ingelheim Chemicals Inc. (Petersburg, VA, USA). The microscope cover glass of diameter 24 mm was purchased from Fisher Scientific Inc. (Pittsburg, USA). Dichloromethane (organic solvent, ACS grade) was obtained from Fisher Scientific Inc. (Pittsburg, PA). All materials and chemicals were used as received without further purification. MCF-7 cells were maintained in minimum essential medium, Eagle with Earle's balanced salt solution (MEM) (ATCC, Manassas, VA) supplemented with 0.05% Insulin (2 mg mL^{-1}), 1% fungizone, 1% penicillin–streptomycin (P/S) solution, and 10% fetal bovine serum (FBS). The anticancer drug, doxorubicin hydrochloride was purchased from Sigma Aldrich. 0.25% trypsin-EDTA (Invitrogen) and Dulbecco's phosphate buffered saline (DPBS) (Cellgro, Mediatech Inc, Manassas, USA) were used as received. For all cell culture experiments, 70–80% confluent cells in a T-25 flask were used.

Synthesis of "Breath Figure" PLGA: Breath figure method and coating techniques were combined to fabricate porous thin PLGA filmswith various pore size ranges. Prior to coating, the cover glass was acid-treated and UV-sterilized for an hour.

Spin-Coating Procedure: A manual spin coater (WS-400–6NPP-LITE, Laurell Technologies Corporation, North Wales, PA) was used to fabricate a thin film on the glass substrate in the presence of moist air (Figure 1). The spin coater was connected with a tube from which the humid air stream was passed into the coating chamber throughout the coating process. By bubbling air continuously through the distilled water, the humidity (≈70% relative humidity [RH]) was created and maintained.[21] The PLGA polymer was first dissolved in dichloromethane at a concentration of 10% (w/v). Then, the polymer solution (≈0.8 mL) was dropped onto the glass substrate and immediately accelerated to 2500 rpm for 30–40 s to spread the solution uniformly over the substrate. The solvent was evaporated out quickly and thereby, facilitating water droplets to condense from the humid air to create porous cavities into the polymer film. Macroscopically, the initial transparent polymer solution turned opaque due to the emulsification of water droplets in the breath figure process. The samples were then dried for at least a day at room temperature (RT) before using them for cell culture experiment.

Dip-Coating Procedure: In the case of dip coating, the polymer solution (10%, w/v, in dichloromethane) was taken in a glass beaker (Figure 1). Using a tweezer, the glass substrate was dipped into the polymer solution. After allowing the substrate to coat with the polymer film for about 10–20 s, the substrate was removed and transferred into the closed chamber maintained with constant humidity (≈70% RH). Inside the chamber, the coated substrate was placed in a slanting position in a glass petri-dish. This step was followed by blowing humid air for 30 min to an hour. Samples were then dried at room temperature for at least a day. The film formed on the unexposed (bottom) side of the cover glass was peeled off and discarded once the polymer was sufficiently dried. In contrast to spin coating (<10 μm pores), the evaporation of solvent is slow and steady during the dip coating procedure, which results into increased condensation and penetration of water droplets into the polymer (>10 μm pores).

Preparation of 2D Substrate: To compare the results of cell culture on porous PLGA, we used a microscope cover glass and non-porous PLGA films as 2D control samples. The non-porous PLGA was prepared similarly using the spin-coating procedure under nitrogen atmosphere (<10% RH). In order to promote cell adhesion, the glass cover slips were initially treated with 1 N HCl solution for 30 min to an hour, rinsed thoroughly with distilled water, and stored in absolute ethanol. Prior to using them for cell culture or coating with the polymer, they were either air dried or heated over a flame to evaporate off the ethanol. All PLGA samples (both porous films) and the cover glass were UV-sterilized for an hour and conditioned with the cell culture medium (MEM) overnight at 37 °C in an incubator before plating the MCF-7 cells.

Characterization of Breath Figure PLGA Films: Surface and cross-sectional morphologies of PLGA samples (spin-coated, dip-coated, and non-porous films) were characterized by scanning electron microscopy (SEM; Hitachi Field Emission S-4800) operated at an accelerating voltage of 3 kV. The samples were subjected to sputtering (Polaron SEM sputter) with a thin gold layer (15 mA, 2.4 kV, 90 s) prior to SEM imaging. To obtain the side view, a cross-sectional cut of the film was gold coated as well. Imaging software (Image-pro Plus version 5.0) was used to measure average pore size and pore size distributions. A minimum of five SEM images (obtained from three different experiments) were used in analysis to count 300 pore dimensions to arrive at the statistics on pore size distributions.

Cell Culture on Breath Figure PLGA Films and 2D Controls: Spin- or dip-coated porous PLGA films, and the cover glass with non-porous 2D PLGA films were placed in six-well tissue culture plates for preconditioning. The schematic of cell seeding and growth is depicted in Figure 1. For all cultures, the seeding density was 5×10^4 cells per well unless indicated otherwise. Detailed accounts appear in the Supporting Information.

Microscopic Analysis of Cell Morphology and Growth on Breath Figure PLGA Films and 2D Controls: The morphology of cells seeded in both 2D and breath figure samples was assessed by toluidine blue staining, SEM and confocal laser scanning microscope analysis. For visualizing the morphological changes, fixed MCF-7 cells grown on various substrates were stained with 0.5% toluidine blue solution (Polyscientific R&D Corp., NY, USA) for 10–15 min.

Analysis of Ductal Outgrowth Morphology: Individual cysts/acinar units at different regions of the polymer matrix were imaged in whole mounts of the day 7 culture preparations by confocal microscopy with a 20× objective (Leica TCS SP2). Growth on 2D coverslips was also examined using the same procedures. Serial optical sections were taken sequentially from the surface through the whole thickness of the acinar units on various films. The average pattern and thickness of the branching structures was generated by stacking and color-coding multiple (≈15–50 depending on the thickness of the growth) images of a lobular unit stained with K18 and DAPI. These optical sections were stacked to give maximum projected image of all ductal and lobular units within this area using Leica software. Only those outgrowth that had a distinctive appearance as branched units with lumen containing lobular units were chosen for analyses. Thickness of growth in projected confocal images was also measured through z-stacks imaging. Numerical results were analyzed using the Mann–Whitney rank sum test.

Proliferation of MCF-7 Cells on Breath Figure PLGA and 2D Surface: To study the effect of porosity on cell proliferation, a growth kinetics study using trypan blue assay (0.4% solution, Sigma Aldrich) was performed over a period of 8 d. Briefly, 2.5×10^4 MCF-7 cells/well were cultured on preconditioned porous polymers (both spin coated and dip coated) and on control 2D glass coverslips. After overnight attachment, the substrates were transferred to fresh six-well plates. As defined earlier, this time point was designated as day zero for quantitation. Cell counting was carried out with trypan blue on hemocytometer. For each time interval (days 0, 1, 3, 4, 5, 6, and 8), triplicate samples (separate well plates for each time interval) were examined to obtain at least six

measurements. It may be noted that detaching cells from the polymers required twice the amount of trypsin than what was required to remove cells from the 2D cover glass.

RNA Isolation and PCR Analysis: To study the gene expression profile of cells grown on breath figure PLGA and 2D samples, cells from the various samples were harvested using 0.25% trypsin-EDTA solution. Total RNA from these cells was then extracted using TRIzol reagent (1 mL reagent per one million cells approximately) (Invitrogen) as per the manufacturer's instructions. Details of reaction conditions are available in the Supporting Information.

Doxorubicin Treatment on MCF-7 Cells: The effect of doxorubicin, an anti-cancer chemotherapeutic agent, on the proliferation of cells cultured on breath figure PLGA and 2D cover glass environment was examined using the Alamar blue cell viability assay. Unlike the other assays, a total of 5×10^3 MCF-7 cells were plated per well of a six-well plate for this assay. The reason to seed with a smaller number of cells was to allow them to stay in log phase for a longer period of time without reaching confluence. The desired drug concentrations (0.5×10^{-6} and 5×10^{-6} M of doxorubicin hydrochloride) were prepared by diluting the stock drug solution in MEM cell culture medium. The first doxorubicin treatment was given after 5 d of cell culture. For untreated control samples, dimethyl sulfoxide (DMSO, Sigma–Aldrich, volume equivalent used for preparing 5×10^{-6} M doxorubicin) was used. Fresh media containing the appropriate concentration of the drugs was replenished every 72 h. The Alamar blue assay was performed according to manufacturer protocols (Invitrogen, Carlsbad, CA) on days 5, 8, and 11 after plating the cells. Briefly, the Alamar blue reagent (100 µL) was added to cultures; following incubation for 4 h at 37 °C, treated samples were pipetted out in triplicates into a fresh 96-well black plate. The absorbance was recorded using a FLx800 Fluorescence microplate reader (Biotek Instruments, Inc). In relation to DMSO treated control samples, the percentage (normalized) of viable cells for the drug treated samples was calculated.

Statistical Analysis: All experiments were carried out in triplicate or as indicated otherwise. Data are expressed as mean ± standard deviation. Statistical significance was determined using Students two-tailed paired *t*-test or Mann–Whitney rank sum test. Differences were considered statistically significant for values of $p \leq 0.05$.

Supporting Information

Supporting Information is available from the Wiley Online Library or from the author.

Acknowledgements

The authors thank Pallavi S. Dhule for assisting with the drug treatment experiment, and Courtney Lopreore for help with the confocal microscopy at the Coordinated Instrumentation Facility at Tulane University. Support from the Department of Defense under Grant No. W81XWH-10–1–0377 and DoD (PC080811), and the Louisiana Cancer Research Consortium, is gratefully acknowledged.

Received: May 14, 2013
Revised: August 6, 2013
Published online: October 17, 2013

[1] B. Weigelt, M. J. Bissell, *Semin. Cancer Biol.* **2008**, *18*, 311.
[2] M. J. Bissell, V. M. Weaver, S. A. Lelievre, F. Wang, O. W. Petersen, K. L. Schmeichel, *Cancer Res.* **1999**, *59*, 1757.
[3] S. Krause, M. V. Maffini, A. M. Soto, C. Sonnenschein, *Tissue Eng. Part C Methods* **2008**, *14*, 261.
[4] J. J. Campbell, C. J. Watson, *Organogenesis* **2009**, *5*, 43.
[5] K. M. Yamada, E. Cukierman, *Cell* **2007**, *130*, 601.
[6] J. B. Kim, *Semin. Cancer Biol.* **2005**, *15*, 365.
[7] M. Hakanson, M. Textor, M. Charnley, *Integr. Biol.* **2011**, *3*, 31.
[8] J. L. Horning, S. K. Sahoo, S. Vijayaraghavalu, S. Dimitrijevic, J. K. Vasir, T. K. Jain, A. K. Panda, V. Labhasetwar, *Mol. Pharm.* **2008**, *5*, 849.
[9] H. K. Dhiman, A. R. Ray, A. K. Panda, *Biomaterials* **2004**, *25*, 5147.
[10] S. W. Kang, Y. H. Bae, *Biomaterials* **2009**, *30*, 4227.
[11] X. Wang, L. Sun, M. V. Maffini, A. Soto, C. Sonnenschein, D. L. Kaplan, *Biomaterials* **2010**, *31*, 3920.
[12] P. A. Kenny, G. Y. Lee, C. A. Myers, R. M. Neve, J. R. Semeiks, P. T. Spellman, K. Lorenz, E. H. Lee, M. H. Barcellos-Hoff, O. W. Petersen, J. W. Gray, M. J. Bissell, *Mol. Oncol.* **2007**, *1*, 84.
[13] A. Nyga, U. Cheema, M. Loizidou, *J. Cell Commun. Signal* **2011**, *5*, 239.
[14] Y. S. Torisawa, H. Shiku, T. Yasukawa, M. Nishizawa, T. Matsue, *Biomaterials* **2005**, *26*, 2165.
[15] S. Krause, M. V. Maffini, A. M. Soto, C. Sonnenschein, *BMC Cancer* **2010**, *10*.
[16] T. R. Sodunke, K. K. Turner, S. A. Caldwell, K. W. McBride, M. J. Reginato, H. M. Noh, *Biomaterials* **2007**, *28*, 4006.
[17] H. K. Dhiman, A. R. Ray, A. K. Panda, *Biomaterials* **2005**, *26*, 979.
[18] Y. Markovitz-Bishitz, Y. Tauber, E. Afrimzon, N. Zurgil, M. Sobolev, Y. Shafran, A. Deutsch, S. Howitz, M. Deutsch, *Biomaterials* **2010**, *31*, 8436.
[19] M. Srinivasarao, D. Collings, A. Philips, S. Patel, *Science* **2001**, *292*, 79.
[20] A. Bolognesi, C. Mercogliano, S. Yunus, M. Civardi, D. Comoretto, A. Turturro, *Langmuir* **2005**, *21*, 3480.
[21] T. Ponnusamy, L. B. Lawson, L. C. Freytag, D. A. Blake, R. S. Ayyala, V. T. John, *Biomatter* **2012**, *2*, 77.
[22] U. H. F. Bunz, *Adv. Mater.* **2006**, *18*, 973.
[23] Y. Zhu, R. Sheng, T. Luo, H. Li, J. Sun, S. Chen, W. Sun, A. Cao, *ACS Appl. Mater. Interfaces* **2011**, *3*, 2487.
[24] Y. Fukuhira, E. Kitazono, T. Hayashi, H. Kaneko, M. Tanaka, M. Shimomura, Y. Sumi, *Biomaterials* **2006**, *27*, 1797.
[25] M. Tanaka, *Biochim. Biophys. Acta* **2011**, *1810*, 251.
[26] M. Tanaka, K. Nishikawa, H. Okubo, H. Kamachi, T. Kawai, M. Matsushita, S. Todo, M. Shimomura, *Colloids Surf. A Physicochem. Eng. Asp.* **2006**, *284*, 464.
[27] S. K. Sahoo, A. K. Panda, V. Labhasetwar, *Biomacromolecules* **2005**, *6*, 1132.
[28] C. Fischbach, R. Chen, T. Matsumoto, T. Schmelzle, J. S. Brugge, P. J. Polverini, D. J. Mooney, *Nat. Methods* **2007**, *4*, 855.
[29] Y. Yang, S. Basu, D. L. Tomasko, L. J. Lee, S. T. Yang, *Biomaterials* **2005**, *26*, 2585.
[30] A. L. Pollack, R. B. Runyan, K. E. Mostov, *Dev. Biol.* **1998**, *204*, 64.
[31] M. J. Williams, P. Clark, *J. Anat.* **2003**, *203*, 483.
[32] N. H. Brown, *Cold Spring Harb. Perspect. Biol.* **2011**, *3*.
[33] P. Lu, K. Takai, V. M. Weaver, Z. Werb, *Cold Spring Harb. Perspect. Biol.* **2011**, *3*.
[34] T. R. Cox, J. T. Erler, *Dis. Model Mech.* **2011**, *4*, 165.
[35] M. J. Bissell, H. G. Hall, G. Parry, *J. Theor. Biol.* **1982**, *99*, 31.
[36] R. B. Weiss, *Semin. Oncol.* **1992**, *19*, 670.
[37] F. Zheng, S. Wang, M. Shen, M. Zhu, X. Shi, *Polym. Chem.* **2013**, *4*, 933.
[38] A. Schreer, C. Tinson, J. P. Sherry, K. Schirmer, *Anal. Biochem.* **2005**, *344*, 76.
[39] F. Zheng, S. Wang, S. Wen, M. Shen, M. Zhu, X. Shi, *Biomaterials* **2013**, *34*, 1402.
[40] F. Liu, R. Guo, M. Shen, X. Cao, X. Mo, S. Wang, X. Shi, *Soft Mater.* **2010**, *8*, 239.
[41] M. Prewitz, F. P. Seib, T. Pompe, C. Werner, *Macromol. Rapid Commun.* **2012**, *33*, 1420.
[42] P. B. Welzel, M. Grimmer, C. Renneberg, L. Naujox, S. Zschoche, U. Freudenberg, C. Werner, *Biomacromolecules* **2012**, *13*, 2349.